Nonlinear Adaptive Parameter Estimation Algorithms for Hysteresis Models of Magnetostrictive Actuators

James M. Nealis [1] and Ralph C. Smith [2]
Department of Mathematics
Center for Research in Scientific Computation
North Carolina State University
Raleigh, NC 27695

Abstract

Increased control demands in applications including high speed milling and hybrid motor design have led to the utilization of magnetostrictive transducers operating in hysteretic and nonlinear regimes. To achieve the high performance capabilities of these transducers, models and control laws must accommodate the nonlinear dynamics in a manner which is robust and facilitates real-time implementation. This necessitates the development of models and control algorithms which utilize known physics to the degree possible, are low order, and are easily updated to accommodate changing operating conditions such as temperature. We consider here the development of nonlinear adaptive identification for low order, energy-based models. We illustrate the techniques in the context of magnetostrictive transducers but they are sufficiently general to be employed for a number of commonly used smart materials. The performance of the identification algorithm is illustrated through numerical examples.

Keywords: Nonlinear parameterization, hysteresis and constitutive nonlinearities, magnetostrictive materials

1. Introduction

Piezoceramic and magnetostrictive transducers are finding increased use in high performance applications due to their set point accuracy and high bandwidth capabilities. However, they also exhibit hysteresis and constitutive nonlinearities which must be accommodated to achieve design specifications. At low frequencies and moderate drive levels, these effects can often be mitigated through feedback loops. At high drive levels or high frequencies, however, the hysteresis and nonlinear dynamics must be incorporated into models and subsequent control designs. In this paper, we consider the development of a nonlinear adaptive parameter estimation algorithm for updating parameters in energy-based hysteresis models.

To illustrate, consider the prototypical magnetostrictive actuator depicted in Figure 1. Input stresses and displacements are provided by the Terfenol-D rod in response to fields generated by the surrounding solenoid. As detailed in [1, 2], such actuators have the capability of generating broadband, high force, responses. However, they also exhibit varying degrees of hysteresis and nonlinearities in the relation between the input field H, the magnetization M and strains λ in the Terfenol-D rod. We employ this transducer design as a template for developing the nonlinear adaptive estimation techniques discussed here but we note that the models and estimation techniques are sufficiently general to permit direct extension to analogous piezoelectric and ferroelectric models of the type developed in [7, 9].

[1] Email: jmnealis@unity.ncsu.edu, Telephone: (919) 515-8968
[2] Email: rsmith@eos.ncsu.edu; Telephone: (919) 515-7552

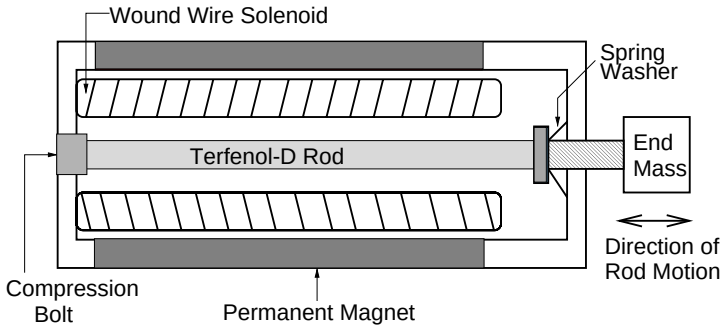

Figure 1. Prototypical magnetostrictive transducer.

There exist a number of techniques for modeling hysteresis in magnetostrictive materials including Preisach models [10, 12] and domain wall models [1, 2]. As illustrated in [11, 12], Preisach models can, under approximation, be linearly parameterized in terms of coefficients to be identified thus permitting the use of linear adaptive algorithms. This advantage is often offset, however, by the large number of required nonphysical parameters and the extensions to the theory required to accommodate temperature and frequency dependence. The domain wall models are low order and have physical parameters but exhibit a nonlinear dependence on the parameters. In this paper, we extend the techniques of [3, 4] to obtain nonlinear adaptive estimation laws for updating parameters in these domain wall models.

A significant difficulty in developing a nonlinear parameter adaptation law is the fact that gradient update methods are not always sufficient for estimating nonlinearly occurring parameters. To illustrate, consider an error model of the form

$$\dot{e} = -ke + f(\phi, \theta) - f(\phi, \widehat{\theta})$$

where e is the error between the desired and the measured trajectories. We denote the measurable states as ϕ, $k > 0$ is a scalar, θ is a nonlinearly occurring parameter, $\widehat{\theta}$ is the parameter estimate and f is a scalar valued nonlinear function. Consider the gradient update law

$$\dot{\widehat{\theta}} = e \nabla f_{\widehat{\theta}}.$$

With the standard Lyapunov function, $V = \frac{1}{2}(e^2 + \tilde{\theta}^2)$, where $\tilde{\theta} = \widehat{\theta} - \theta$, we see that

$$\dot{V} = -ke^2 + e\left[f(\phi, \theta) - f(\phi, \widehat{\theta}) + \tilde{\theta} \nabla f_{\widehat{\theta}}\right].$$

If $e < 0$, it is necessary that $\nabla f_{\widehat{\theta}}(\theta - \widehat{\theta}) \leq f(\phi, \theta) - f(\phi, \widehat{\theta})$ which implies that f is convex. If $e > 0$, then f must be concave to ensure $\dot{V} \leq 0$. We observe the gradient method does not ensure stability for all $\widehat{\theta}$. A gradient method applied to a nonlinear parameterized system may not only be insufficient but may lead to instability. The method we discuss here does not strictly rely on a gradient rule but differs depending on the sign of the error [3, 4].

In Section 2 we summarize the hysteresis and transducer model. In Section 3 we review the nonlinear adaptive method for the scalar case. In Section 4 we present an extension of the method to the vector case. Section 5 provides numerical examples of both the scalar and vector cases.

2. Transducer Model

We summarize here the model developed in [1, 2] for magnetostrictive transducers operating in nonlinear and hysteretic regimes. This model is formulated in two steps: (i) quantification of anhysteretic magnetization, M_{an} and (ii) quantification of the total magnetization, M.

One source of hysteresis occurs in the relationship between an applied magnetic field H and the resulting magnetization M in the Terfenol-D. Domain wall theory is based on the concept that domain walls are present

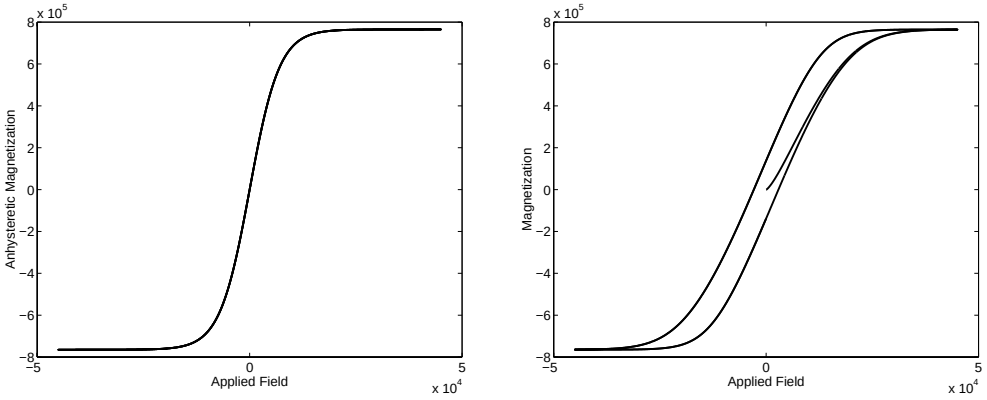

(a) (b)

Figure 2. (a) Anhysteretic magnetization; (b) Total magnetization.

in the material and pinned at inclusions. Physically, the anhysteretic magnetization M_{an} can be thought of as the magnetization obtained when domain walls are translated across pinning sites with no loss of energy. The anhysteretic magnetization depends on the effective field given by $H_e = H + \alpha M$ where α quantifies the effects of the interdomain coupling. Under the assumption of constant stress, we balance thermal and magnetostrictive energy via Boltzmann principles. The anhysteretic magnetization can be given by either the Langevin model

$$M_{an} = M_s \left(\coth\left(\frac{H_e}{a}\right) - \frac{a}{H_e} \right) \tag{1}$$

or the Ising model

$$M_{an} = M_s \tanh\left(\frac{H_e}{a}\right) \tag{2}$$

depending on the assumptions we make on the orientation of dipoles. Here M_s is the saturation magnetostriction and a is a temperature dependent coefficient. The two anhysteretic models are equivalent to third order. Since the parameter a is closely effected by the temperature, we will chose to update a in the nonlinear adaptive parameter estimation. The ability to adapt a to varying conditions would be extremely useful since the temperature is difficult to regulate in many industrial applications. For example, in the transducer depicted in Figure 1, the current in the solenoid can cause Ohmic heating and effect the value of a.

To quantify the total magnetization, we incorporate the irreversible magnetization M_{irr} due to domain wall translation. Magnetostatic principals are used to compute the energy required to reorient dipoles, as detailed in [1, 2]. This yields the differential equation

$$\frac{\partial M_{irr}}{\partial H} = \hat{\delta} \frac{M_{an} - M_{irr}}{k\delta - \alpha(M_{an} - M_{irr})} \ . \tag{3}$$

Here $\delta = sign(dH)$ to ensure the pinning is opposite the change in magnetization and $\hat{\delta}$ is 0 if $dH > 0$ and $M > M_{an}$ or $dH < 0$ and $M < M_{an}$ and 1 otherwise. This indicator is necessary to model the physical observation that, after a field reversal, the changes in magnetization are purely reversible until the anhysteretic value is reached. The parameter k quantifies the average energy required to translate a domain wall.

The reversible magnetization M_{rev} is due to domain wall bending. As detailed in [1, 2], the reversible magnetism is given by the algebraic relationship

$$M_{rev} = c(M_{an} - M_{irr}) \tag{4}$$

where c is a material parameter which quantifies the reversibility of the material. The total magnetism is then

$$M = (1 - c)M_{irr} + cM_{an} \ . \tag{5}$$

The relation (5) is typically employed for material characterization. For the purposes of nonlinear parameterization, we reformulate (5) as

$$\frac{\partial M}{\partial H} = F(H, M) \tag{6}$$
$$M(H_0) = M_0$$

where

$$F(H,M) = \frac{1}{1 + c\alpha \frac{\partial}{\partial H} M_{an}} \left[\hat{\delta} \frac{M_{an} - M}{k\delta - \hat{\alpha}(M_{an} - M)} + c \frac{\partial}{\partial H} M_{an} \right] \tag{7}$$

with $\hat{\alpha} = \dfrac{\alpha}{1-c}$. The anhysteretic and total magnetization are illustrated in Figure 2.

The model developed in (5) or (6) quantifies the hysteretic relationship between the imposed field and the resulting magnetization. Next, we need to quantify the strains, forces, and displacements generated by the changes in magnetization. We do this in two steps: (i) quantify the free strains in the material and (ii) quantify the total strains which include elastic effects. We present a brief overview of the model of the full transducer dynamics. For a more complete derivation see [2].

We characterize the free strain, or magnetostriction, for a Terfenol-D actuator by the quadratic relation

$$\lambda(t) = \frac{3\lambda_s}{2M_s^2} M^2(t) \tag{8}$$

where λ_s denotes the saturation magnetostriction. To achieve bidirectional strains or forces, the transducer is biased by a surrounding magnet or the application of a DC field to the solenoid. For a bias of $M_s/2$, the free strain is modeled by

$$\lambda(t) = \frac{3\lambda_s}{2M_s^2} \left[M^2(t) + 2M_s M(t) \right]. \tag{9}$$

Once we have quantified the magnetostriction that occurs in response to an applied field, we must incorporate the materials elastic properties. We assume one end of the rod ($x = 0$) to be fixed while the other end ($x = L$) is constrained by a damped oscillator and has a point mass attached (see Figure 3). The internal damping coefficient, density, Young's Modulus and point mass are given by c_D, ρ, E, and M_ℓ, respectively. The damping spring is assumed to have stiffness k_ℓ and Kelvin-Voigt damping coefficient c_ℓ.

If we assume linear elasticity, Kevin-Voigt damping and small displacements, then the stress at any point x, $0 \le x \le L$, is given by

$$\sigma(t,x) = E \frac{\partial u}{\partial x}(t,x) + c_D \frac{\partial^2 u}{\partial x \partial t}(t,x) - E\lambda(t) \tag{10}$$

where $u(t,x)$ is the longitudinal displacement. We assume that the magnetostriction given by (9) is independent of position. This independence is reasonable since flux shaping via the surrounding magnet can be used to minimize end effects in the rod which results in uniform magnetostriction along the rod. Force balancing then yields

$$\rho A \frac{\partial^2 u}{\partial t^2} = \frac{\partial N_{tot}}{\partial x} \tag{11}$$

where the resultant is specified given by

$$N_{tot}(t,x) = EA \frac{\partial u}{\partial x}(t,x) + c_D A \frac{\partial^2 u}{\partial x \partial t}(t,x) - EA\lambda(t)\ . \tag{12}$$

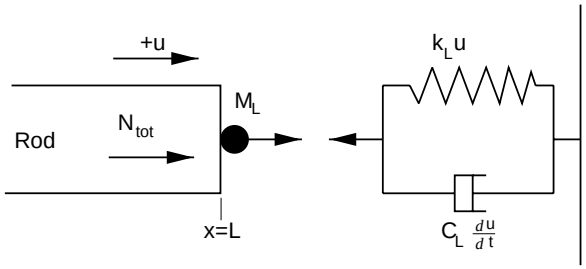

Figure 3. Rod approximation model.

To obtain appropriate boundary conditions, we first note that $u(t,0) = 0$. We balance forces at $x = L$ to give

$$N_{tot}(t,L) = -k_\ell u(t,L) - c_\ell \frac{\partial u}{\partial t}(t,L) - M_\ell \frac{\partial^2 u}{\partial x \partial t}(t,L).$$

We take the initial conditions to be $u(0,x) = 0$ and $\dfrac{\partial u}{\partial x}(0,x) = 0$. We can now use a Galerkin finite element to numerically approximate the solution to the PDE (11).

We specified the magnetostriction $\lambda(t)$ to be independent of spatial location due to the design of the surrounding permanent magnet. This implies that the dynamics of the transducer which are currently modeled by a PDE can be accurately approximated by a damped spring mass system

$$\widehat{G}(s) = \frac{1}{ms^2 + ks + c} = \frac{w}{s^2 + \hat{k}s + \hat{c}} \ . \tag{13}$$

We examined the poles and zeros of the transfer functions which resulted from a Galerkin finite element approximation with varying number of basis elements. We found the model could be adequately approximated by one with two poles and no zeros for any number of basis elements. We used the poles and gain of these transfer functions to developed the damped spring mass model for the transducer dynamics. The parameters for the resulting model (13) were determined to be $w = 1.3724 \times 10^{-2}$, $\hat{k} = 7.8899 \times 10^3$ and $\hat{c} = 6.4251 \times 10^7$.

3. Nonlinear Adaptive Parameter Estimation

We wish to adaptively estimate and update the nonlinearly occurring parameter a in the hysteretic model (6) to model the effects of changing temperatures. To accomplish this, we consider the theory in [3, 4] and develop modifications required for the hysteresis model employed here. One criterion for the algorithm is the capability to obtain estimates of a which are sufficiently accurate to maintain tolerances specified for the transducers (e.g., cutting tolerances of $\pm$ .001 in). Furthermore, the algorithm must be stable and persistent excitation conditions must be established to ensure convergence.

The nonlinear parameterization assumes all of the states are available and identifies parameters for a system of the form

$$\dot{y} = -ky + af(u(t), \theta)$$

where $k > 0$ is a scalar and $\theta \in \mathbb{R}^m$ is an unknown parameter, $\theta \in \Theta$ where Θ is the bounded region in which θ lies. The function f is taken to be a scalar valued nonlinear function of the input $u(t)$. As motivated by [3, 4], we consider the estimation algorithm

$$\begin{aligned}
\dot{\widehat{y}} &= -k\widehat{y} - \epsilon \ \mathrm{sat}(\tfrac{\bar{y}}{\epsilon}) + af(u,\widehat{\theta}) - a^* \mathrm{sat}\left(\tfrac{\bar{y}}{\epsilon}\right) \\
\dot{\widehat{\theta}} &= -\tilde{y}_\epsilon \phi^* \\
\tilde{y}_\epsilon &= \tilde{y} - \epsilon \ \mathrm{sat}\left(\tfrac{\bar{y}}{\epsilon}\right) \\
\tilde{y} &= \widehat{y} - y
\end{aligned} \tag{14}$$

where $\epsilon > 0$, $\mathrm{sat}(\cdot)$ is a saturation function defined as

$$\mathrm{sat}(x) = \begin{cases} 1, & x \geq 1 \\ x, & |x| < 1 \\ -1, & x \leq 1 \end{cases}$$

and a^* and ϕ^* are the solution of

$$\begin{aligned}
a^* &= \min_{\phi \in \mathbb{R}^m} \max_{\theta \in \Theta} \ g(\theta, \phi) \\
\phi^* &= \arg \min_{\phi \in \mathbb{R}^m} \max_{\theta \in \Theta} \ g(\theta, \phi) \\
g(\theta,\phi) &= a \ \mathrm{sat}(\tfrac{\bar{y}}{\epsilon}) \left[f(u,\widehat{\theta}) - f(u,\theta) - \phi^T(\widehat{\theta} - \theta) \right] \ .
\end{aligned} \tag{15}$$

We note that when $|\tilde{y}| < \epsilon$, the adaptation of the parameters stops, imposing what is termed a dead-zone. The method will continue to adapt the parameters until the magnitude of the error $\tilde{y}$ is less than the given ϵ.

We consider the min/max algorithm (15) to handle the regions of nonconvexity of f where the gradient method is insufficient. The use of a tuning error $\tilde{y}_\epsilon$ rather than a tracking error $\tilde{y}$ ensures continuity of the adaptation as does the use of a saturation function over that of a signum function [4]. We do not need the assumption that the parameters and the parameter estimates are bounded for stability, but rather to compute the closed form solution of (15).

If we define $\tilde{\theta} = \widehat{\theta} - \theta$ and $x = [\tilde{y}, \tilde{\theta}^T]^T$, then we can show that the system (14) is stable with $x = 0$ by proving that $V = e^2 + a\tilde{\theta}^2$ is a Lyapunov function. Following theory outlined in [5], we first note that $\dot{V} = 2\tilde{y}_\epsilon \dot{\tilde{y}}_\epsilon + 2a\tilde{\theta}\dot{\tilde{\theta}}$. If $|\tilde{y}| \leq \epsilon$ then $\tilde{y}_\epsilon = 0$ which implies $\dot{V} = 0$. We then need to show that $\dot{V} \leq 0$ if $|\tilde{y}| > \epsilon$. We can express $\dot{V}$ as

$$\begin{aligned}
\dot{V} &= 2\tilde{y}_\epsilon(-k\widehat{y} - \epsilon \text{ sat}\left(\tfrac{\bar{y}}{\epsilon}\right) + af(u,\widehat{\theta}) - a^*\text{sat}\left(\tfrac{\bar{y}}{\epsilon}\right) + ky - af(u,\theta)) - 2a\tilde{\theta}\tilde{y}_\epsilon\phi^* \\
&= -2k\tilde{y}_\epsilon\ \tilde{y} + 2\tilde{y}_\epsilon(af(u,\widehat{\theta}) - af(u,\theta) - a\tilde{\theta}\phi^* - \epsilon \text{ sat}\left(\tfrac{\bar{y}}{\epsilon}\right) - a^*\text{sat}\left(\tfrac{\bar{y}}{\epsilon}\right)) \\
&= -2k\tilde{y}_\epsilon\tilde{y} + 2\tilde{y}_\epsilon\left[a(f(u,\widehat{\theta}) - f(u,\theta) - \tilde{\theta}\phi^*) - \epsilon \text{ sat}\left(\tfrac{\bar{y}}{\epsilon}\right) - a^*\text{sat}\left(\tfrac{\bar{y}}{\epsilon}\right)\right] .
\end{aligned}$$

If $\tilde{y} > 0$, then $\text{sat}\left(\frac{\bar{y}}{\epsilon}\right) = 1$ so we must have

$$a^* \geq a \text{ sat}\left(\frac{\tilde{y}}{\epsilon}\right)(f(u,\widehat{\theta}) - f(u,\theta) - \tilde{\theta}\phi^*) - \epsilon \text{ sat}\left(\frac{\tilde{y}}{\epsilon}\right) \text{ for all } \theta \in \Theta .$$

This implies that we can let

$$a^* = a \max_{\theta\in\Theta} \text{ sat}\left(\frac{\tilde{y}}{\epsilon}\right)(f(u,\widehat{\theta}) - f(u,\theta) - \tilde{\theta}\phi^*) \text{ for any } \phi^*$$

so by the definition of ϕ^* and a^* the inequality is satisfied and hence $\dot{V} \leq 0$. If $\tilde{y} < 0$, then $\text{sat}\left(\frac{\bar{y}}{\epsilon}\right) = -1$ so we must have

$$a^* \geq -\left[a(f(u,\widehat{\theta}) - f(u,\theta) - \tilde{\theta}\phi^*) + \epsilon\right] \text{ for all } \theta \in \Theta$$

or

$$a^* \geq a \text{ sat}\left(\frac{\tilde{y}}{\epsilon}\right)\left[f(u,\widehat{\theta}) - f(u,\theta) - \tilde{\theta}\phi^*\right] + \epsilon \text{ sat}\left(\frac{\tilde{y}}{\epsilon}\right) \quad \text{for all } \theta \in \Theta .$$

We can again let

$$a^* = a \max_{\theta\in\Theta} \text{ sat}\left(\frac{\tilde{y}}{\epsilon}\right)\left[f(u,\widehat{\theta}) - f(u,\theta) - \tilde{\theta}\phi^*\right] \quad \text{for any } \phi^*$$

so by the definition of ϕ^* and a^* the inequality is satisfied again and hence $\dot{V} \leq 0$.

To implement the method proposed in the system (14), it is necessary to solve the min/max problem (15). To do this, we must construct a concave cover $\overline{F}(\theta)$ and a convex cover $\underline{F}(\theta)$ where the covers satisfy

$$\overline{F}(\theta) \geq f - \widehat{f} \qquad \underline{F}(\theta) \leq f - \widehat{f}$$

for $\widehat{f} = f(u,\widehat{\theta})$. The following definitions and construction are summarized from [4].

Definition 1: A point $\theta^0 \in \theta_c$ if $\theta^0 \in \Theta$ and

$$\nabla f_{\theta^0}(\theta - \theta^0) \geq f - f^0$$

where $\nabla f_{\theta^0} \equiv \left.\dfrac{\partial f}{\partial \theta}\right|_{\theta^0}$ and $f^0 = f(\phi, \theta^0)$.

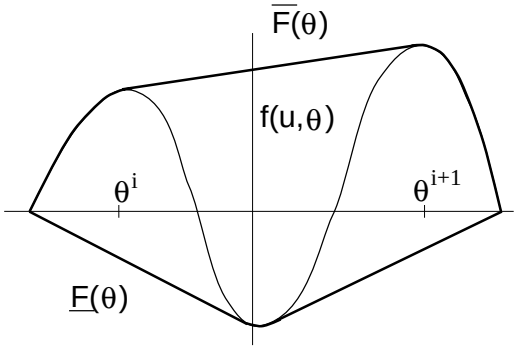

Figure 4. Convex and concave cover of $f(u,\theta)$.

Definition 2: $\tilde{\theta}_c \equiv \overline{\theta}_c \cap \Theta$ where $\overline{\theta}_c$ is the complement of θ_c

If f is not concave on Θ, then $\tilde{\theta}_c$ is given by $\tilde{\theta}_c = \{\theta^{12}, \theta^{34}, \ldots, \theta^{mn}\}$ where $\theta^{ij} = [\theta^i,\ \theta^j]$ are the regions where f is not concave, $\theta^j \geq \theta^j$. Using Definitions 1 and 2, the concave cover of $f - \widehat{f}$ on Θ can be constructed as

$$\overline{F}(\theta) = \begin{cases} f - \widehat{f}, & \text{for all } \theta \in \theta_c \\ \theta^{ij}\theta + c^{ij}, & \text{for all } \theta \in \theta^{ij} \in \tilde{\theta}_c \end{cases} \tag{16}$$

where

$$\theta^{ij} = \frac{f^j - f^i}{\theta^j - \theta^i}, \qquad c^{ij} = f^i - \hat{f} - \theta^{ij}\theta^i, \qquad f^i = f(\phi, \theta^i)\ .$$

Similarly, we construct a convex cover of $f - \widehat{f}$ by defining

$$\begin{aligned} \theta_v &\equiv \{\theta^0 \mid \nabla f_{\theta^0}(\theta - \theta^0) \leq f - f^0\} \\ \tilde{\theta}_v &\equiv \overline{\theta}_v \cap \Theta \end{aligned}$$

$$\underline{F}(\theta) = \begin{cases} f - \widehat{f}, & \text{for all } \theta \in \theta_v \\ \theta^{ij}\theta + c^{ij}, & \text{for all } \theta \in \theta^{ij} \in \tilde{\theta}_v\ . \end{cases} \tag{17}$$

Once we have constructed $\underline{F}(\theta)$ and $\overline{F}(\theta)$, a closed form solution to the min/max problem (15) is given by

$$\begin{aligned} a^* &= \overline{F}(\widehat{\theta}) \\ \theta^* &= \begin{cases} \nabla f_{\widehat{\theta}},\ \text{if } \widehat{\theta} \in \theta_c & \text{if } \tilde{y}_\epsilon > 0 \\ \theta^{ij},\ \text{if } \widehat{\theta} \in \theta^{ij} \in \tilde{\theta}_c \end{cases} \\ a^* &= -\underline{F}(\widehat{\theta}) \\ \theta^* &= \begin{cases} \nabla f_{\widehat{\theta}},\ \text{if } \widehat{\theta} \in \theta_v & \text{if } \tilde{y}_\epsilon < 0\ . \\ \theta^{ij},\ \text{if } \widehat{\theta} \in \theta^{ij} \in \tilde{\theta}_v \end{cases} \end{aligned} \tag{18}$$

A proof that (18) is the solution to (15) can be found in [4].

Having established the stability of the adaptation method by the Lyapunov function stated earlier, now we seek sufficient conditions which establish uniform asymptotic stability of the system (14). We summarize the condition for convergence of the parameters and tracking error in the following theorem presented in [3].

Theorem 1: If for every $t_1 > t_0$, there exists $T_0,\ \epsilon_0,\ \delta_0$, and a subinterval $[t_2,\ t_2+\delta_0] \in\ [t_1,\ t_1+T_0]$ such that

$$\beta \int_{t_2}^{t_2+\delta_0} \left[(t_2) f(u,\widehat{\theta}(t_2)) - f(u,\theta)\right]\ d\tau \geq 2\epsilon + \epsilon_0 ||\tilde{\theta}(t_2)|| \ , \tag{19}$$

then the origin $x = 0$ is uniform asymptotically stable.

In Theorem 1, $\beta = 1$ if $f(u,\widehat{\theta})$ is convex and $\beta = -1$ if $f(u,\widehat{\theta})$ is concave. We notice several differences between this condition and the condition for a linear parameterization. The sign of the integral is important. The sign is not strictly determined by $f(u,\widehat{\theta}) - f(u,\theta)$ but also by the convexity or concavity of f as indicated by β. This coupling arises from the min/max algorithm and is necessary but not sufficient to ensure that the method will leave the dead zone, $|\tilde{y}| \leq \epsilon$. The integral must be sufficiently large to leave the deadzone, which necessitates the term incorporating ϵ on the right hand side of (19).

We placed the excitation conditions on f in Theorem 1. We wish to derive conditions on $u(t)$ since we have some freedom when choosing $u(t)$. Theorem 1 does not give conditions on the input u to satisfy the inequality (19) nor does it guarantee that such an input exists. Inequality (19) includes two components. First, the magnitude of the integrand must be sufficiently large. For a large parameter error the input must be such that the difference between the function evaluated at the actual parameter and the parameter estimate is adequately large. We chose an input signal which drives the function f to a level where a change in the parameter is most noticeable. Secondly, the integral must be the same sign as β. This coupling states that if f is convex, then the integrand should be positive. If f is concave, then the integrand should be negative. The min/max feature of the algorithm gives stability but an acceptable input must be used to guarantee parameter convergence. Parameter convergence is ensured by updating using the gradient information and we must pick an input signal accordingly.

To ensure parameter convergence, we can summarize the conditions on u as either

(a) For the given $\tilde{\theta}$, u must reverse the sign of the integrand of (19) while keeping the convexity/concavity of f fixed.

or

(b) For the given $\tilde{\theta}$, u must reverse the convexity/concavity of f, while preserving the sign of the integrand of (19).

(see [4]).

4. Matrix Equation Case

Since many physical systems with inherent hysteresis are modeled by higher order equations, we extend here the scalar method proposed in [3, 4] to systems of equations. We stated previously that, due to transducers design and field shaping, the smart structure can be modeled to first approximation as damped spring mass system. Therefore, for our magnetostrictive transducer application, the identification method must work for at least a second order system. To utilize the method for matrix equations, we must redefine several variables in the scalar case. We wish to use the solution to the min/max problem (15), so we must ensure that we do not alter that aspect of the formulation.

We consider here the parameter identification for the matrix system

$$\dot{y} = Ay + Bf(u,\theta) \ .$$

Here we assume that A is diagonal with eigenvalues λ_i. Since our smart system is strongly damped, we have the real part of the eigenvalues in the left half plane. We define

$$\begin{aligned}
\dot{\widehat{y}} &= A\widehat{y} + Bf(u,\widehat{\theta}) - C\left[\epsilon\ \mathrm{sat}(\tfrac{\bar{y}}{\epsilon})) + a^* \mathrm{sat}\left(\tfrac{\bar{y}}{\epsilon}\right)\right] \\
\tilde{y} &= \mathrm{Re}\sum_{i=1}^{N} (\widehat{y} - y)_i \\
\dot{\widehat{\theta}} &= -\tilde{y}_\epsilon \phi^* \\
\tilde{y}_\epsilon &= \tilde{y} - \epsilon\ \mathrm{sat}\left(\tfrac{\bar{y}}{\epsilon}\right)
\end{aligned} \tag{20}$$

where $C = [0, \cdots, 0, 1] \in \mathbb{R}^N$, N is the number of states, and a^* and ϕ^* are the solutions of

$$\begin{aligned} a^* &= \min_{\phi \in \mathbb{R}^m} \max_{\theta \in \Theta} g(\theta, \phi) \\ \phi^* &= \arg \min_{\phi \in \mathbb{R}^m} \max_{\theta \in \Theta} g(\theta, \phi) \\ g(\theta, \phi) &= b \text{ sat} \left(\frac{\tilde{y}}{\epsilon} \right) \left[f(u, \widehat{\theta}) - f(u, \theta) - \phi^T (\widehat{\theta} - \theta) \right] \end{aligned} \tag{21}$$

where $b = \sum_{i=1}^{N} B_i$. It is important to note that the solution to the min/max problem (21) is a scalar multiple of the solution to (15).

We must prove that this adaptive parameter estimation method is stable. We consider the Lyapunov candidate

$$V = \tilde{y}_\epsilon^2 + b\tilde{\theta}^2$$

which yields

$$\dot{V} = 2\tilde{y}_\epsilon \dot{\tilde{y}}_\epsilon + 2b\tilde{\theta}\dot{\widehat{\theta}}$$

with

$$\dot{\tilde{y}}_\epsilon = \text{Re} \left[\sum_{i=1}^{N} \left(A(\tilde{y} - y) + B(\hat{f} - f) - C \left(\epsilon \text{ sat}(\frac{\tilde{y}}{\epsilon}) + a^* \text{sat} \left(\frac{\tilde{y}}{\epsilon} \right) \right) \right) \right] .$$

This can be written as

$$\dot{\tilde{y}}_\epsilon = \text{Re} \left[\sum_{i=1}^{N} \lambda_i (\tilde{y} - y) \right] + B(\hat{f} - f) - C \left(\epsilon \text{ sat}(\frac{\tilde{y}}{\epsilon}) + a^* \text{sat} \left(\frac{\tilde{y}}{\epsilon} \right) \right)$$

which yields

$$\begin{aligned} \dot{V} &= 2\tilde{y}_\epsilon \text{Re} \left[\sum_{i=1}^{N} \lambda_i (\tilde{y} - y) \right] + 2\tilde{y}_\epsilon \left[b(\hat{f} - f - \tilde{\theta}\phi^*) - \epsilon \text{ sat}(\tfrac{\tilde{y}}{\epsilon}) - a^* \text{sat} \left(\tfrac{\tilde{y}}{\epsilon} \right) \right] \\ \dot{V} &= 2\tilde{y}_\epsilon \text{Re} \left[\sum_{i=1}^{N} \lambda_i \tilde{y} - \sum_{i=1}^{N} \lambda_i y \right] + 2\tilde{y}_\epsilon \left[b(\hat{f} - f - \tilde{\theta}\phi^*) - \epsilon \text{ sat}(\tfrac{\tilde{y}}{\epsilon}) - a^* \text{sat} \left(\tfrac{\tilde{y}}{\epsilon} \right) \right] . \end{aligned}$$

Since $\text{Re}(\lambda_i) < 0$ for all i, we have

$$\text{Re} \left[\sum_{i=1}^{N} \lambda_i \tilde{y} \right] \leq \overline{\lambda} \left[\sum_{i=1}^{N} \tilde{y} \right] \qquad , \qquad \text{Re} \left[\sum_{i=1}^{N} \lambda_i y \right] \leq \overline{\lambda} \left[\sum_{i=1}^{N} y \right] \tag{22}$$

where $\overline{\lambda} = \max_i \text{Re}(\lambda_i)$. Using these inequalities we obtain

$$\dot{V} \leq 2\overline{\lambda}\tilde{y}\tilde{y}_\epsilon + 2\tilde{y}_\epsilon \left[b(\hat{f} - f - \tilde{\theta}\phi^*) - \epsilon \text{ sat}(\frac{\tilde{y}}{\epsilon}) - a^* \text{sat} \left(\frac{\tilde{y}}{\epsilon} \right) \right] .$$

We complete the proof by using the definitions of a^* and ϕ^* as the solutions of (21) in a manner analogous to that of the proof in Section 3. One item in the proof we must note is that the inequalities in (22) are true only for specific input functions $u(t)$. The input signal we use is a monotonically increasing function . Therefore the states y and $\tilde{y}$ are positive. If we desire a different input signal, it would be necessary to re-examine the inequalities in (22).

5. Numerical Examples

We provide a scalar and matrix example to demonstrate the capabilities of the nonlinear adaptive parameter estimation method. We consider first the scalar model. We specify the dynamics of the system by

$$\dot{y} = -ky + M(u, a) \tag{23}$$

where $M(u, a)$ is the solution of the domain wall model (5) or (6) for the hysteretic material. We assume the parameter estimate $\widehat{a}$ to be bounded such that $\widehat{a} \in [6300,\ 7300]$ with $\widehat{a}(0) = 6800$. We take the actual value of a to be 7012 A/m and the remaining constants are given as $k = 4000$ A/m, $\alpha = -.01$, $P_s = 7.65 \times 10^5$ A/m, $c = .18$ and $\lambda_s = 1.005 \times 10^{-3}$. One difficulty of the adaptive parameter estimation algorithm is constructing an input $u(t)$ which will provide persistent excitation. Because of the condition imposed for excitation, we use a signal that does not cause the function to change signs. Empirically, it has been established that a monotonically increasing or saturation type input provides accurate results and quick convergence. We chose the input signal, $u(t)$, as an increasing linear function which drives the hysteresis to a level near saturation. This signal provides persistent excitation as well as evaluates the hysteresis model at levels which most noticeably differ according to the parameter a. Figure 5a illustrates the integrand of (19) for a given value of $\tilde{\theta}$ to show that the second condition for persistent excitation is met. The integrand remains positive while switching the convexity/concavity of the function M as seen in Figure 5b. Figure 6 illustrates the ability of the scalar nonlinear parameter estimation method to accurately identify the unknown parameter a. Figure 6a shows the evolution of the parameter estimates which converges quickly to the actual value of 7012. The speed of convergence of the parameter estimation is a notable result since we can potentially combine this identification method with a control technique. The Figure 6b provides a graph of the tracking error $\tilde{y}$. For a given ϵ specified in design tolerances (e.g. cutting accuracy of $\epsilon = 0.001$ in) the method is able to track within an error of ϵ given the conditions of persistent excitation are satisfied. We have empirically noticed the choice of ϵ affects the rate of convergence and the range of parameter estimate values which the method achieves. This gives us a design consideration associated with the tracking accuracy required.

We now consider the matrix system parameter estimation algorithm. The system is a damped spring mass system which models the transducer dynamics of the smart transducer given by (13). Again, we take the function f as the hysteresis model (6) and the parameter a is updated to model its temperature dependence. Figure 7a illustrates the convergence of the estimate to the actual parameter value. Figure 7b depicts the tracking error of the adaptive system. We have successfully extended the parameter identification to matrix systems as seen by the convergence of the parameter and the decay of the tracking error.

For the matrix system there exist a variety implementation issues. The model we consider must be solved numerically. No implicit method can be used because of the unknown forcing function at the next time step. This uncertainty requires the time step to be sufficiently small to ensure accurate solutions of the model given in (13). Any inaccuracy of the solution of (13) can cause the value of $\tilde{y}$ to have a discontinuous jump from positive to negative values. This phenomena causes the min/max solution to jump between utilizing the convex cover

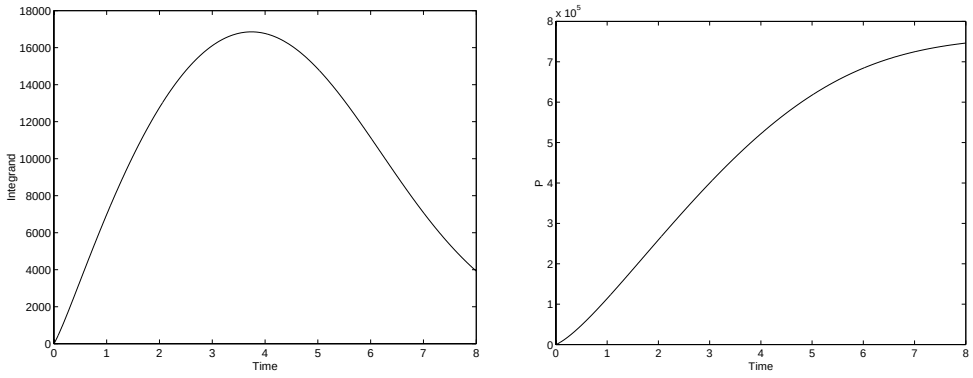

(a) (b)

Figure 5. (a) Value of integrand of Inequality (19); (b) Value of $M(u, \widehat{a})$.

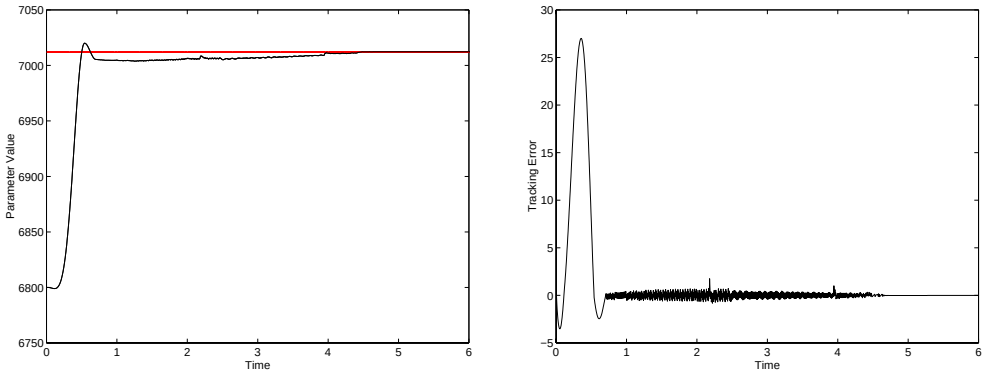

(a) (b)

Figure 6. (a) Parameter estimate; (b) Tracking error for scalar case.

and concave cover. These jumps in turn cause highly oscillatory behavior in the parameter update. We also observed the convergence to be moderately slower with the matrix system than that of the scalar case. However, the convergence rate is still reasonable for a large number of industrial applications.

6. Concluding Remarks

We have formulated the nonlinear adaptive estimation technique of [3, 4] in the context of a nonlinear hysteresis model for magnetostrictive transducers and have extended the theory to the vector case commensurate with these models. Numerical examples illustrate the capability of the method for updating the temperature dependent parameter a to simulate the effect of changing temperature in the transducer. While developed in the context of a model for magnetostrictive materials, the unified nature of the models (see [8]) permits direct extension of the technique to hysteresis models for piezoelectric, relaxor ferroelectric, and shape memory compounds.

One direction of current research focuses on the extension of the algorithms to simultaneously identify multiple parameters; e.g. $\theta = [a,\ k,\ \alpha,\ P_s,\ c]$. While the min/max theory is the same, issues concerning the identification of the convex and concave regions require resolution.

A second direction of current research addresses the development of adaptive and robust control techniques which utilize these models and estimation algorithms. While adaptive control techniques have been developed for models with linear parameterizations [11, 12], analogous convergence criteria for nonlinear models, of the

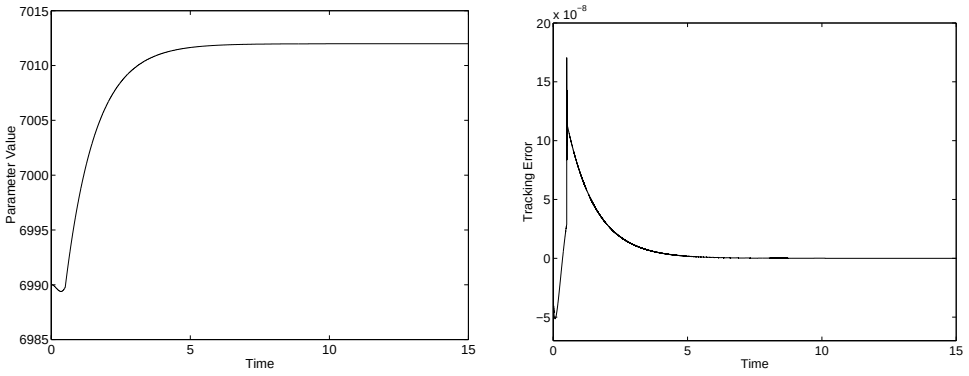

(a) (b)

Figure 7. (a) Parameter estimate; (b) Tracking error for matrix case.

type considered here, have yet to be established. One technique which has been numerically and experimentally implemented is based on the use of partial of full inverse compensators based on approximate inverses to the models [5, 6]. In this case, the adaptive estimation algorithms presented here would be used to update parameters in the model and its inverse. The inverse is then employed in a hybrid controller comprised of feedback and feedforward components. This permits an indirect adaptive updating of the controller to accommodate changing operating conditions.

Acknowledgments

This research was supported in part by the Air Force Office of Scientific Research under the grant AFOSR-F49620-01-1-0107.

References

[1] F.T. Calkins, R.C. Smith and A.B. Flatau, "An Energy-based Hysteresis Model for Magnetostrictive Transducers," *IEEE Transactions on Magnetics*, **36**(2), pp. 429-439, 2000.

[2] M.J. Dapino, R.C. Smith and A.B. Flatau, "A Structural Strain Model for Magnetostrictive Transducers," *IEEE Transactions on Magnetics*, **36**(3), pp. 545-556, 2000.

[3] A. Kojic, C. Cao and A. M. Annaswamy, "Parameter Convergence in systems with Convex/Concave Parameterization," *Proceedings of the 2000 American Control Conference*, pp. 2240-2244, 2000.

[4] A-P Loh, A. M. Annaswamy and F. P. Skantze, "Adaptation in the Presence of a General Nonlinear Parameterization: An Error Model Approach," *IEEE Transactions on Automatic Control*, **44**(9), pp. 1634-1652, 1999.

[5] J. Nealis and R.C. Smith ,"Partial Inverse Compensation Techniques for Linear Control Design in Magnetostrictive Transducers," *Proceedings of the SPIE, Smart Structures and Materials, 2001*, Vol. 4326, pp. 462-473, 2001.

[6] R.C. Smith, C. Bouton and R. Zrostlik, "Partial and Full Inverse Compensation for Hysteresis in Smart Material Systems," *Proceedings of the 2000 American Control Conference*.

[7] R.C. Smith and C.L. Hom, "A Domain Wall Theory for Ferroelectic Hysteresis," *Journal of Intelligent Material Systems and Structures*, **10**(3), pp. 195-213, 1999.

[8] R.C. Smith and J.E. Massad, "A Unified Methodology for Modeling Hysteresis in Ferroic Materials," *Proceedings of the 18th ASME Biennial Conference on Mechanical Vibration and Noise*, to appear.

[9] R.C. Smith and Z. Ounaies, "A Domain Wall Model for Hysteresis in Piezoelectric Materials," *Journal of Intelligent Material Systems and Structures*, **11**(1), pp. 62-79, 2000.

[10] X. Tan, R. Venkataraman and P.S. Krishnaprasad, "Control of Hysteresis: Theory and Experimental Results," *Smart Structures and Materials 2001, Modeling, Signal Processing and Control in Smart Structures*, SPIE Vol. 4326, pp. 101-112, 2001.

[11] G. Tao and P.V. Kokotovic, "Adaptive Control of Plants with Unknown Hysteresis," *IEEE Transactions on Automatic Control*, **40**(2), pp. 200-212, 1995.

[12] G. Tao and P.V. Kokotovic, *Adaptive Control of Systems with Actuator and Sensor Nonlinearities*, John Wiley and Sons, New York, 1996.